Sensitivity of Tropical Tropospheric Temperature to Sea Surface Temperature Forcing

Hui Su, J. David Neelin and Joyce E. Meyerson

Introduction

During El Niño, there are substantial tropospheric temperature anomalies across the entire tropical band associated with the warming of sea surface temperature (SST) in the central and eastern Pacific. What is the relationship between tropical tropospheric temperature response and SST forcing? What is the most important contribution in setting these tropospheric temperature anomalies? Does the relatively small region which has warm SST anomalies added to high climatological SST dominate? Or is it more dependent on the whole region of warm SST anomalies? The Quasi-equilibrium Tropical Circulation Model (QTCM) forced with subregions of SST anomalies is used to investigate the mechanisms for tropical tropospheric temperature anomalies during ENSO.

Quasi-equilibrium Tropical Circulation Model (V2.2):

The QTCM is an intermediate complexity atmospheric circulation model that makes use of properties of a "quasi-equilibrium moist convective closure". It includes nonlinear advection, Betts-Miller convective adjustment, cloud-radiative interaction, and a simple land model.

General Approach

In addition to simulations with observed SST from 1987 - 1998, we conducted simulations with specified SST distributions based on climatological SST plus subregions of SST anomalies observed during an El Niño event. For each distribution, ensemble mean of 10 simulations with slightly different initial conditions are constructed. Anomalies are defined by subtracting the ensemble mean of 10 control runs with climatological SST. The responses in precipitation and tropospheric temperature anomalies are examined. Because the tropospheric temperature response extends throughout the tropics even when SST anomaly forcing is localized, the behavior of the tropical average value is of interest.

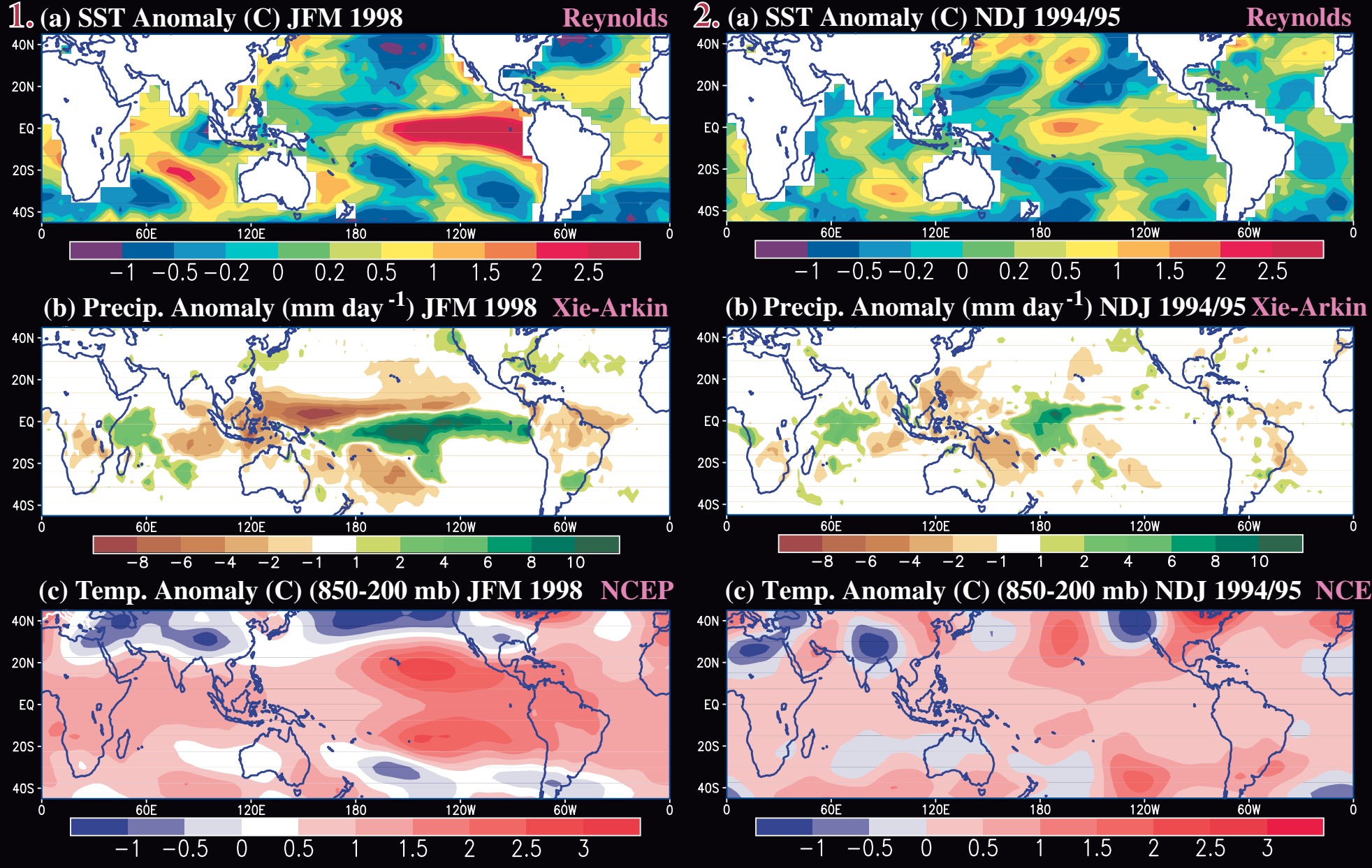

Figure 1. Observed (a) sea surface temperature (SST) in C, (b) precipitation in mm/day and (c) tropospheric temperature (850-200 mb average) anomalies in C for January-March 1998.
Figure 2. As in Fig. 1 but for November 1994 - January 1995.

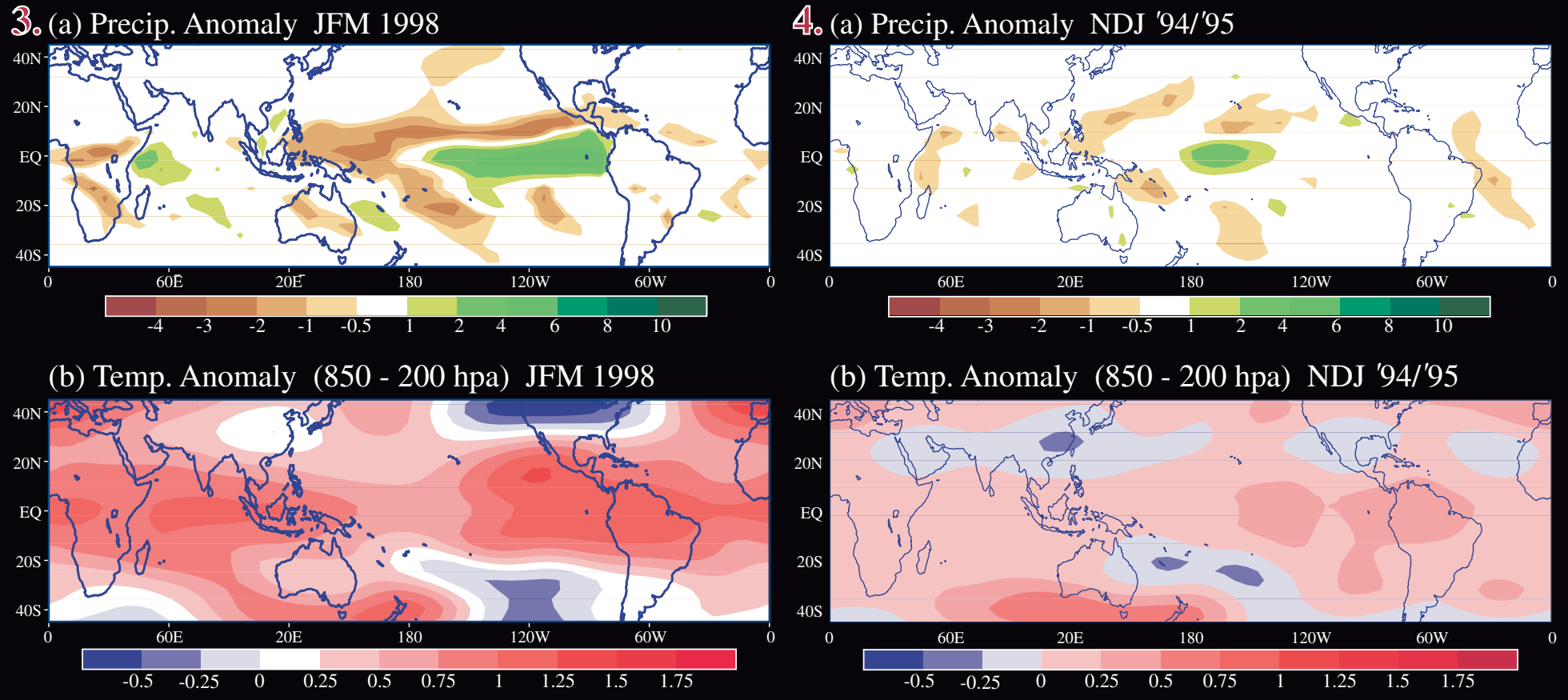

Figure 3. Model-simulated precipitation (mm/day) and tropospheric temperature (850-200mb average, in C) anomalies for JFM 1998 from the run using observed SST from 1982-1998.
Figure 4. As in Fig. 1 but for NDJ 1994/95.

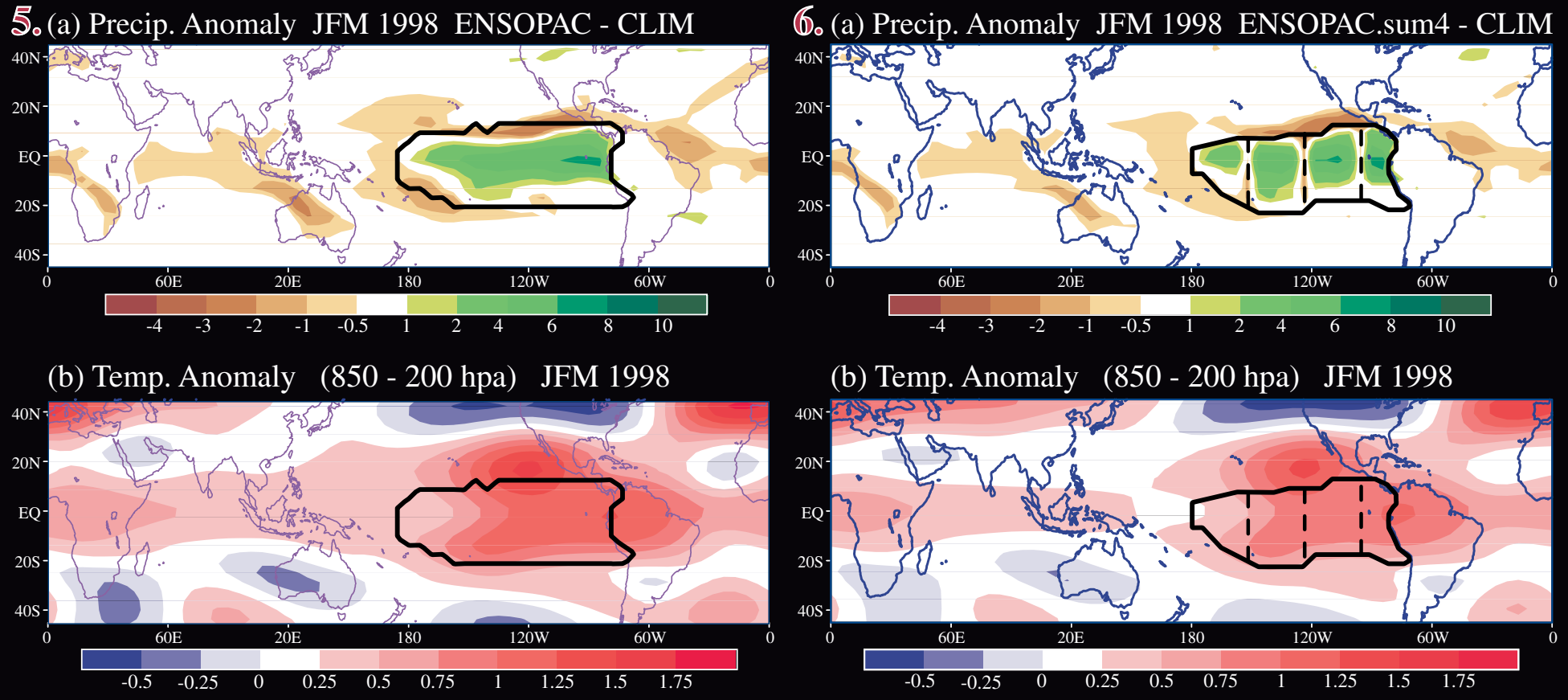

Figure 5. QTCM response to positive SST anomalies during JFM 1998. The JFM positive-only portion of the SST anomalies are specified in the region indicated by a dark outline. (a) Precipitation anomaly (mm/day). (b) Tropospheric temperature (850-200mb average) in C.

Figure 6. The sum of QTCM response to each of the four subregions of positive SST anomalies during JFM 1998. The four subregions are indicated by dark outlines. (a) Precipitation anomaly (mm/day). (b) Tropospheric temperature (850-200mb average) in C.

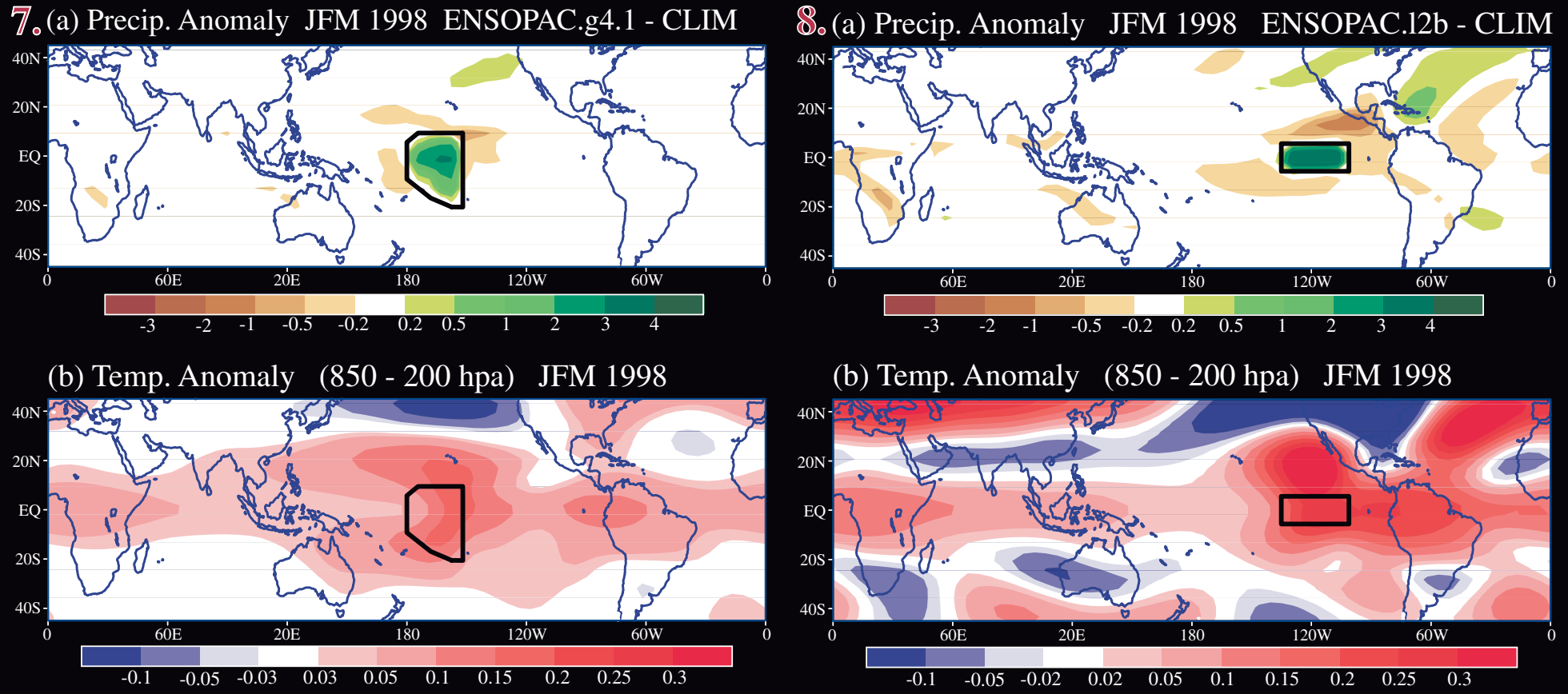

Figure 7. QTCM response to one of the four subregions of positive SST anomalies during JFM 1998. The subregion is indicated by a dark outline. (a) Precipitation anomaly (mm/day). (b) Tropospheric temperature (850-200mb average) in C.

Figure 8. QTCM response to a small subregion of positive SST anomalies taken from the JFM 1998 El Niño case. The subregion is indicated by a dark outline. (a) Precipitation anomaly (mm/day). (b) Tropospheric temperature (850-200mb average) in C.

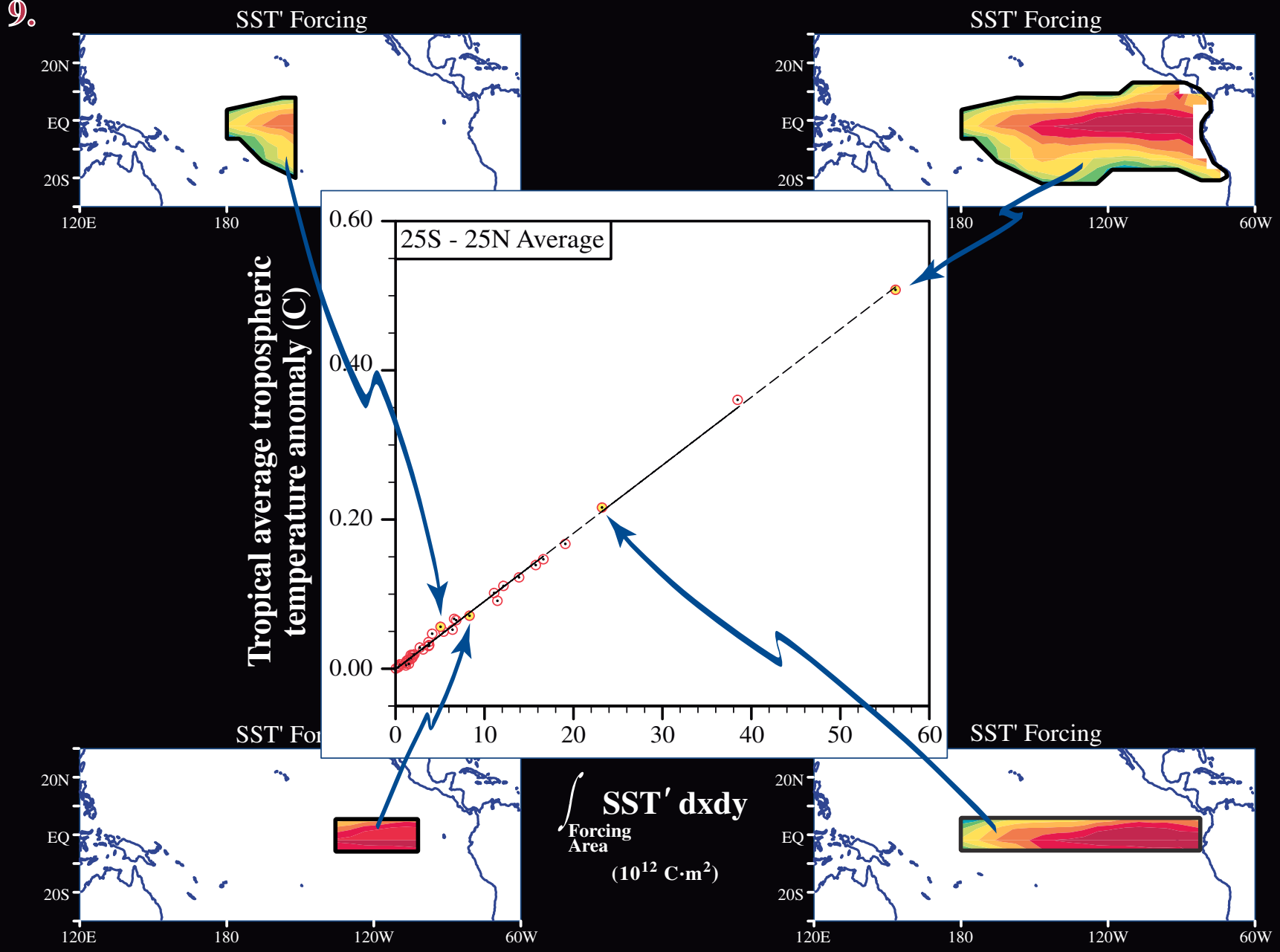

Figure 9. Tropical averaged (25S-25N) tropospheric temperature anomalies versus the spatial integral of SST anomaly forcing for a number of experiments with subregions of the 1998 JFM El Niño SST anomaly. The side-panels show examples of the SST anomaly forcing used in the experiments.

10.

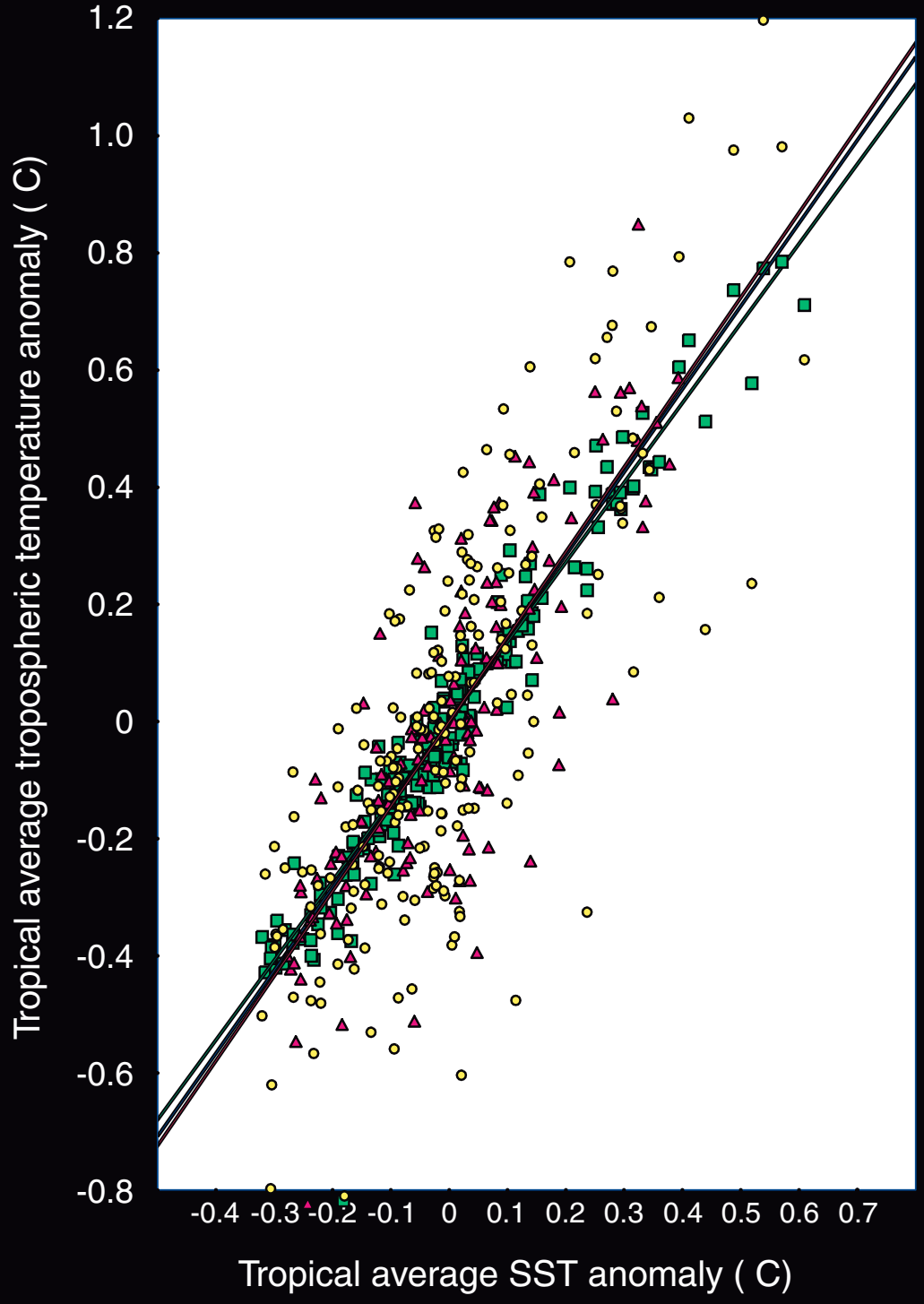

Figure 10. Tropical averaged (25S-25N) tropospheric temperature anomalies versus tropical averaged SST anomalies for NCAR/NCEP reanalysis (1982-1998), MSU temperature (1993-1998) and QTCM simulation using observed SST from 1982-1998. The solid lines are the linear fits to the three datasets. The slopes of three lines are shown in lower-left corner.

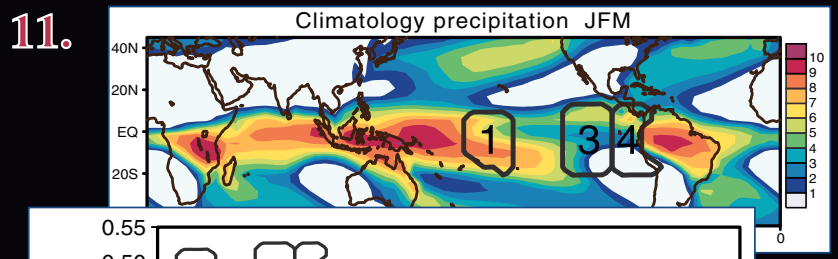

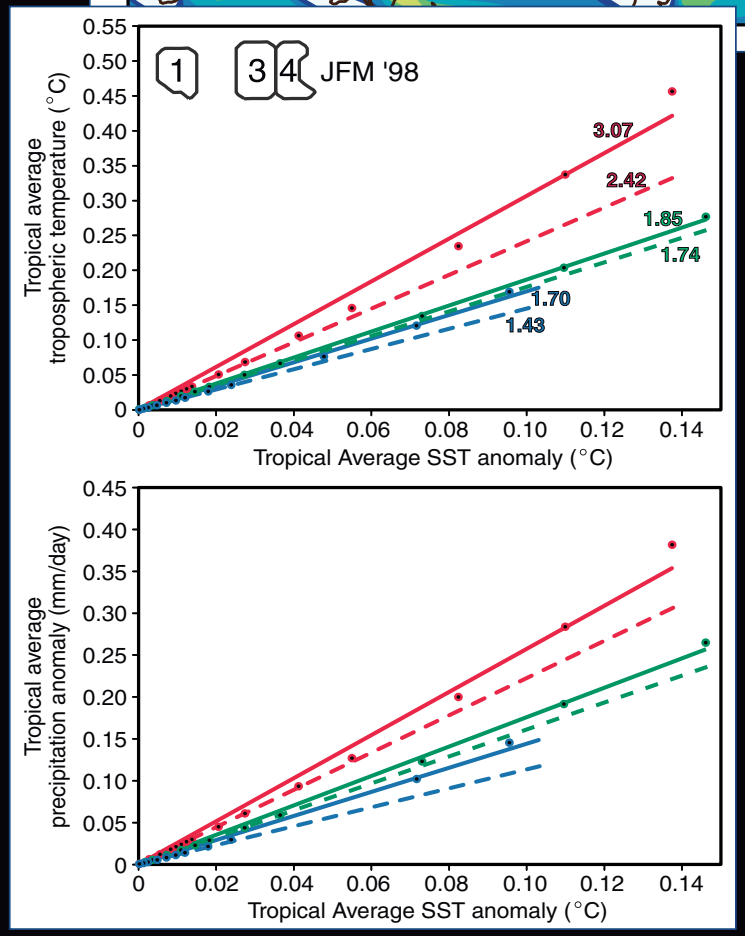

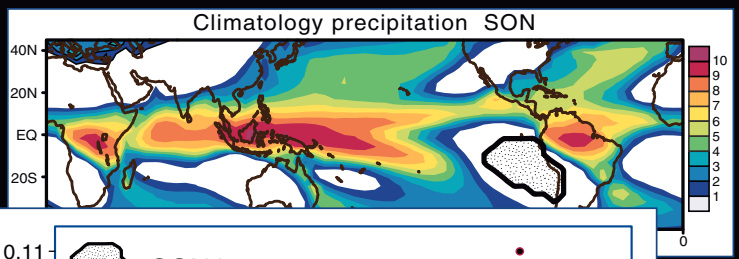

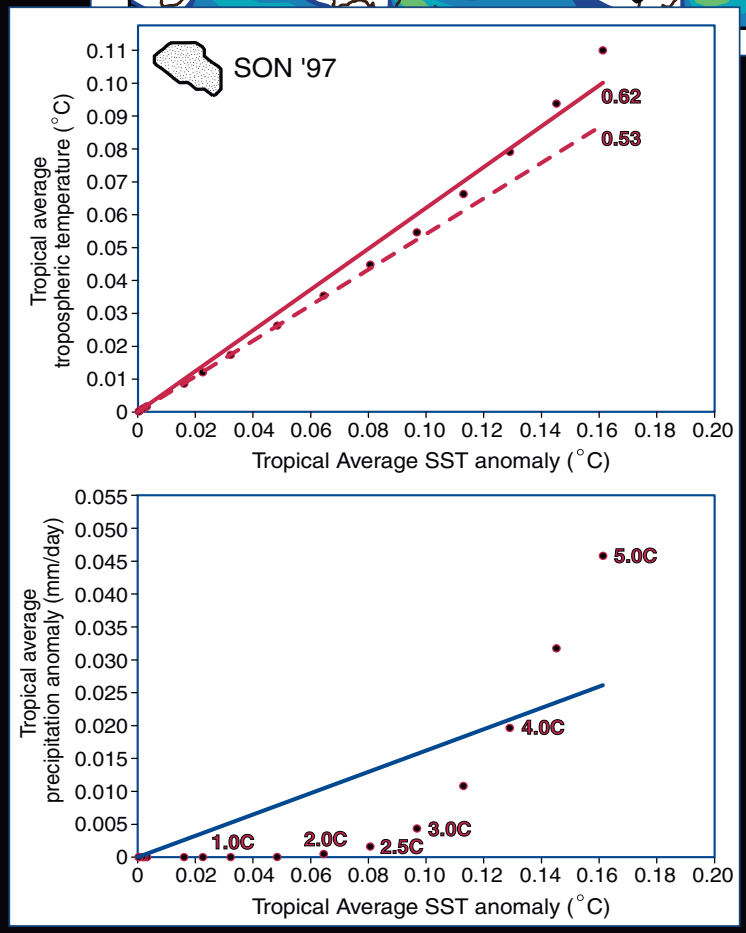

Figure 11. Tropical averaged (25S-25N) tropospheric temperature anomalies and precipitation anomalies versus tropical averaged SST anomalies for simulations with uniform SST anomalies of amplitude 0.01C up to 5C added to climatological SST in three subregions. The regions are indicated by dark outlines and marked 1, 3 and 4 based on the four subregion experiments for the JFM 1998 El Niño. Climatological precipitation during JFM is displayed on top of the figure. Dots show results of the experiments with linear fits given by solid lines. Dashed lines show linearization for small SST anomalies. The numbers next to the linear fits are corresponding slopes.

Figure 12. Same as Fig. 11 but for experiments over a climatologically non-precipitating region, as indicated by dark outline in climatological precipitation map. In the lower panel, numbers next to the dots are the amplitudes of SST anomalies added in the subregion.

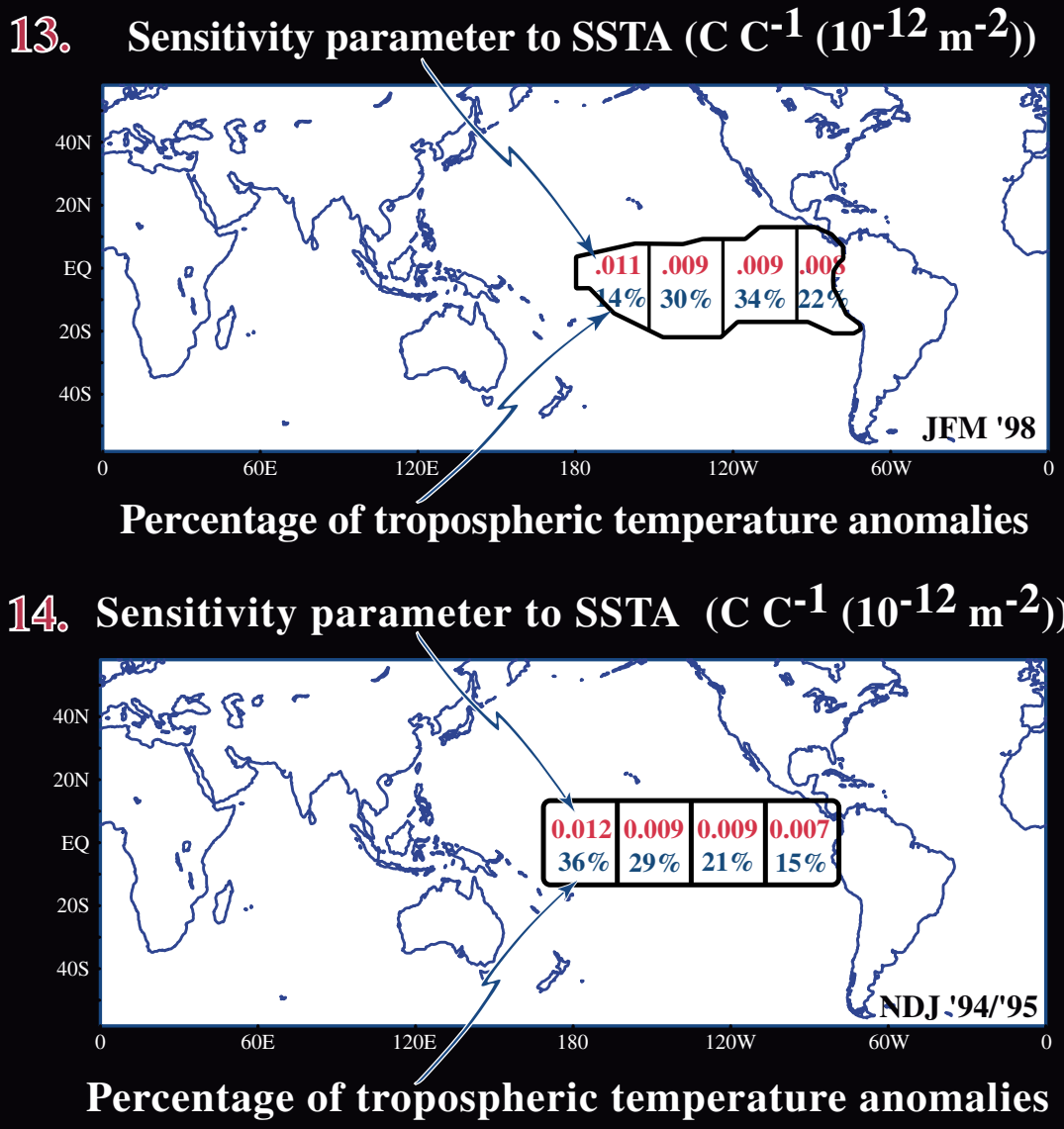

Figure 13. Two measures of the sensitivity parameter of tropical-average tropospheric temperature to SST anomaly in each of four subregions of 1998 JFM positive SST anomalies. The upper numbers are the amount of tropospheric temperature anomalies in degree C per unit SST forcing in $Cx10^{12}$ m^2 (amplitude x area). The lower numbers are the fraction of the average tropospheric temperature anomaly contributed by each subregion.

Figure 14. As in Fig. 11 but for the NDJ 1994/95 case.

Analytical explanation

- Simplifications based on atm. model moist static energy equation
- Main feature: integrating over large regions typical of tropospheric temperature response averages out transport terms

$$\widehat{a}_1(\partial_t+\mathcal{D}_{T1})\,T_1+\widehat{b}_1(\partial_t+\mathcal{D}_{q1})\,q_1+M_1\nabla\cdot\mathbf{v}_1=(g/p_T)\,(F_{rad}+H+E)$$

Consider perturbations from mean state

$$A'=A-\bar{A}$$

Averaged over a large horizontal area

L.H.S. (transport) ≈ 0

$$F'_{rad}+H'+E'\approx 0$$

Net radiative fluxes linear with T'_1, q'_1, T'_s and α'

$$F'_{rad}=\epsilon_{T1}T'_1+\epsilon_{q1}q_{1\prime}+\epsilon_{Ts}T'_s+CRF'$$

Sensible and latent heat fluxes

$$H'=\rho_a C_D\bar{\mathrm{V}}_s\,(T'_s-a_{1s}T'_1)$$

$$E'=\rho_a C_D\bar{\mathrm{V}}_s\,[q'_{sat}(T_s)-b_{1s}q'_1]$$

Cloud radiative forcing as a feedback:

$$CRF'\approx c_tP'\ (c_t=0.06)$$

Precip (convective heating) by moisture budget:

$$P'=M_{q1}\nabla\cdot\mathbf{v}'-\langle\mathbf{v}\cdot\nabla q_1\rangle'+E'$$

Approximate balance

$$\epsilon_{T1}T'_1+\epsilon_{q1}q_{1\prime}+\epsilon_{Ts}T'_s+H'+(1+c_t)E'\approx 0$$

Using

$$\epsilon_{T_1}=-2.89;\ \epsilon_{q_1}=-1.11;\ \epsilon_{T_s}=5.98$$

$$\overline{T}_s=295.0\sim 304.0\ (K),\qquad \overline{\mathrm{V}}_s=5.00\sim 10.0\ (m/s),$$

$$q'_1\approx(0.6\sim 1.6)\,T'_1$$

$$\Rightarrow\qquad \widehat{T}'=\widehat{a}_1T'_1\approx(0.78\sim 2.0)\,T'_s$$

Examples of El Niño simulation

Compared to observations (Fig.1 and Fig. 2), the QTCM reproduces major precipitation and tropospheric temperature responses to El Niño SSTs for a very strong El Niño event, 1997/98 and a relatively weak event, 1994/95 (Fig. 3 and Fig. 4). In Fig 5, only positive SST anomalies in the tropical Pacific from JFM 1998 are used to force the model (run ENSOPAC). It is clear that the ENSOPAC run captures most of the response in precipitation and tropospheric temperature. We then subdivide the positive-only region into subregions and force the model with SST anomalies from each subregion only.

Atmospheric response to subregions of El Niño SST

Figure 6 illustrates the sum of the responses from four subregions of similar size from west to east. The sums of individual runs are similar to the single ENSOPAC run (Fig. 5). However, negative precipitation anomalies are found within the positive SST anomaly region, at the boundaries of the subregions. This is because nonlinear advection effects come into play when strong gradients are artificially created in the subdivision processes. The nonlinear effect is more prominent in precipitation field than the tropospheric temperature field, as the temperature distribution more closely resembles the ENSOPAC experiment. Figure 7 shows the results from one of the four subregions of SST anomaly runs. It is clear that the positive precipitation anomalies are strongly localized to the warm SST anomalies, while the tropospheric temperature displays broad warming in the whole tropical band. Figure 8 is another example of a subdivided SST anomaly experiment, in which only the positive SST anomalies within two degrees of the equator in the central Pacific are retained. Again, the precipitation anomaly is highly localized within the area of positive SST anomaly. The tropospheric temperature anomaly, on the other hand, is spread over a wide region in tropics. The distribution is similar to that of the entire SST anomaly in Fig. 5, although weaker (note the contour interval differs). The temperature anomalies are typical of wave response to localized heating source.

Approximate linearity of tropospheric temperature — Model

As illustrated in Fig. 9, there is a remarkable degree of linearity of the response of tropical tropospheric temperature to El Niño SST anomalies, despite the large range of regional size and spatial patterns sampled. Clearly, it matters how large the area of SST anomaly is, and regions other than the central Pacific do contribute. We note that this applies only to very large-scale aspects of the tropospheric temperature pattern. The precipitation response, for instance, in this model has the same strong nonlinearity at the edges of convection zones seen in observations.

Approximate linearity of tropospheric temperature — Observations

For comparison, we examined the relationship between tropical averaged (25S-25N) tropospheric temperature anomalies versus tropical averaged SST anomalies for NCAR/NCEP reanalysis and Microwave Sounding Unit Channel 2-3 temperature. The results are displayed in Fig. 10 with the QTCM result from the 17 year run from 1982-98. Although the NCEP/NCAR reanalysis and MSU temperature anomalies have more scatter than the model results, the linearity is quite prominent. The slope of the model linear fit is surprisingly close to those of the two independent observational datasets. They are approximately 1.4 C of tropical averaged tropospheric temperature per degree C of tropical averaged SST forcing.

Nonlinearity

In order to further examine the linearity in the tropospheric temperature response to SST forcing, we conducted experiments with uniform SST anomalies of amplitude 0.01 C up to 5 C in specific regions. The results are shown in Fig. 11 and Fig. 12. In Fig. 11, subregion 1 is climatologically precipitating, while regions 3 and 4 are the mixtures of the precipitating and low-precipitation regions. In Fig. 12, the target area is a climatologically non-precipitating region. Over precipitating regions, the linear fits from all experiments of a particular region capture 80-90% of the actual model response. Even the linear fit from the smaller SST anomaly experiments, which corresponds to the analytical linear model predicted temperature response to SST forcing, would produce about 70-80% of the actual model response. The deviation due to nonlinear effects accounts for only 20-30% of the total response. Precipitation response is also largely linear in the three areas. The slopes of tropospheric temperature anomaly versus tropical averaged SST forcing decrease from region 1 to regions 3 and 4. Over a climatologically non-precipitating region (Fig. 12), nonlinearity in precipitation response is dramatic. The tropical averaged precipitation anomalies are virtually zero until the added SST anomalies are more than 2 C and increase more rapidly for large SST anomalies. The tropical averaged tropospheric temperature response is still quite linear for the whole range of SST anomalies.

Sensitivity parameters for subregions

Figure 13 provides two measures of sensitivity parameter of the tropical averaged tropospheric temperature response to tropical SST forcing. The sensitivity is noticeably larger in the central Pacific region where absolute SST is higher, but it does not become small in other regions. Since the middle two of the four regions have larger SST anomalies, these actually contribute more to the JFM 1998 tropospheric temperature anomaly. Similar results are obtained in experiments based on NDJ 94/95 El Niño event (Fig. 14). In this case, the highest percentage contribution came from the subregion in the central Pacific because the warmest SST anomalies were concentrated there. However, the sensitivity parameter over the eastern-most subregion is not small.

Conclusions

- El Niño forced strong precipitation anomalies are local to the origin of positive SST anomalies. On the other hand, tropospheric temperature anomalies spread much further.

- Tropical tropospheric temperature response is approximately linear with the spatial integral of SST forcing → both area coverage and magnitude of SST anomalies matter!

- Nonlinearity in tropical averaged tropospheric temperature response can be modest even when precipitation response is highly nonlinear.

- Subregions of warm SST anomalies contribute fairly evenly to tropospheric temperature anomalies, while regions over climatological warm water (i.e. Central Pacific) are slightly more sensitive.

University of California, Los Angeles
Department of Atmospheric Sciences and
Institute of Geophysics and Planetary Physics

This work was supported in part by National Science Foundation Grant ATM-0082529 and National Oceanographic and Atmospheric Administration Grant NA86-GP0314.